GeroScience (2024) 46:3135–3147
https://doi.org/10.1007/s11357-024-01061-y

ORIGINAL ARTICLE

Impact of knockout of dual-specificity protein phosphatase 5 on structural and mechanical properties of rat middle cerebral arteries: implications for vascular aging

Chengyun Tang · Huawei Zhang · Jane J. Border · Yedan Liu · Xing Fang · Joshua R. Jefferson · Andrew Gregory · Claire Johnson · Tae Jin Lee · Shan Bai · Ashok Sharma · Seung Min Shin · Hongwei Yu · Richard J. Roman · Fan Fan

Received: 7 December 2023 / Accepted: 1 January 2024 / Published online: 10 January 2024

Abstract Vascular aging influences hemodynamics, elevating risks for vascular diseases and dementia. We recently demonstrated that knockout (KO) of *Dusp5* enhances cerebral and renal hemodynamics and cognitive function. This improvement correlates with elevated pPKC and pERK1/2 levels in the brain and kidneys. Additionally, we observed that *Dusp5* KO modulates the passive mechanical properties of cerebral and renal arterioles, associated with increased myogenic tone at low pressure, enhanced distensibility, greater compliance, and reduced stiffness. The present study evaluates the structural and mechanical properties of the middle cerebral artery (MCA) in *Dusp5* KO rats. We found that vascular smooth muscle cell layers and the collagen content in the MCA wall are comparable between *Dusp5* KO and control rats. The internal elastic lamina in the MCA of *Dusp5* KO rats exhibits increased thickness, higher autofluorescence intensity, smaller fenestrae areas, and fewer fenestrations. Despite an enhanced myogenic response and tone of the MCA in *Dusp5* KO rats, other passive mechanical properties, such as wall thickness, cross-sectional area, wall-to-lumen ratio, distensibility, incremental elasticity, circumferential wall stress, and elastic modulus, do not significantly differ between strains. These findings suggest that while *Dusp5* KO has a limited impact on altering the structural and mechanical properties of MCA, its primary role in ameliorating hemodynamics and cognitive functions is likely attributable to its enzymatic activity on cerebral arterioles. Further research is needed to elucidate the specific enzymatic mechanisms and explore potential clinical applications in the context of vascular aging.

Keywords DUSP5 · Vascular mechanical properties · PKC · ERK · AD/ADRD

Chengyun Tang, Huawei Zhang, and Jane J. Border contributed equally to this work.

C. Tang · H. Zhang · J. J. Border · Y. Liu · X. Fang · J. R. Jefferson · R. J. Roman · F. Fan (✉)
Pharmacology & Toxicology, University of Mississippi Medical Center, Jackson, MS, USA
e-mail: ffan@augusta.edu

C. Tang · A. Gregory · C. Johnson · F. Fan
Physiology, Medical College of Georgia, Augusta University, Augusta, GA, USA

T. J. Lee · S. Bai · A. Sharma
Center for Biotechnology and Genomic Medicine, Medical College of Georgia, Augusta University, Augusta, GA, USA

S. M. Shin · H. Yu
Anesthesiology, Medical College of Wisconsin, Milwaukee, WI, USA

Introduction

Vascular aging denotes age-related structural and functional changes in blood vessels. These mechanical alterations in the vasculature influence

hemodynamics, thereby heightening the risk of vascular diseases and dementia [1]. Genetic factors, alongside various other mechanisms such as inflammation, mitochondrial dysfunction, oxidative stress, and telomere attrition, wield considerable influence over vascular aging by modulating vascular structure and hemodynamics [2–10].

Dual-specificity protein phosphatase 5 (DUSP5) is a nuclear enzyme that specifically dephosphorylates the tyrosine-threonine residues of extracellular signal-related kinase 1/2 (ERK 1/2) in the mitogen-activated protein kinase pathway, leading to the inactivation of ERK 1/2 [11–14]. Elevations in phosphorylated protein kinase C (pPKC) and phosphorylated ERK1/2 (pERK1/2) promote calcium influx in vascular smooth muscle cells (VSMCs) and facilitate vasoconstriction. Knockout (KO) of *Dusp5* results in ERK nuclear translocation, which promotes cell proliferation through heightened activities of cell cycle regulatory proteins and posttranslational modifications that enhance pro-survival gene function and reduce cell death [12, 15]. DUSP5 also plays a direct role in promoting cell death in response to endoplasmic reticulum stress [16]. DUSP5 suppresses the actin cytoskeleton rearrangement by negatively modulating the ERK-MLCK-Myosin IIB signaling cascades for its potential antiviral effects [17]. The essential impacts of DUSP5 have been linked to ischemic stroke, hypertension, renal disease, pulmonary hypertension, cancers, osteoarthritis, immunological diseases, and neurodegenerative diseases [18–24]. In human studies, DUSP5 has been reported to regulate hippocampal dentate gyrus plasticity potentially and is associated with late-onset Alzheimer's disease (AD) [25–27].

There is growing evidence suggesting that vascular factors can contribute to the development and progression of Alzheimer's disease and Alzheimer's disease-related dementias (AD/ADRD) [28, 29]. Brain hypoperfusion attributed to impaired cerebral blood flow (CBF) autoregulation, neurovascular uncoupling, blood–brain barrier leakage, and neurodegeneration is important potential causal factors in AD and aging-, hypertension-, and diabetes-related ADRD [4, 30–39]. We have recently documented that *Dusp5* KO amplifies myogenic reactivity and autoregulation of blood flow in both cerebral and renal circulations, concomitant with elevated levels of pERK1/2 and pPKC [11, 12, 23, 40, 41]. Inhibition of ERK and PKC notably boosted the contractile potential of VSMCs obtained from middle cerebral arteries (MCAs), associated with a dose-dependent dilation of the MCAs and penetrating arterioles (PAs), with a more pronounced impact observed in *Dusp5* KO rats [12, 40]. Additionally, there was a noteworthy enhancement in learning and memory observed in *Dusp5* KO rats, suggesting that targeting DUSP5 deletion could hold promise as a therapeutic approach for delaying vascular aging and the onset of AD/ADRD [40]. Furthermore, we examined the impact of *Dusp5* KO on the mechanical characteristics of brain PAs and renal interlobular arterioles. We found that both PAs and renal IAs in *Dusp5* KO rats displayed features of eutrophic vascular hypotrophy, increased myogenic tone, improved distensibility, enhanced compliance, and reduced stiffness, while wall-to-lumen ratios remained unchanged [12].

The present study focused on how the KO of Dusp5 influenced the mechanical vascular characteristics of the MCA, the major blood vessel in the brain susceptible to various vascular disorders [42, 43]. Our study involved a thorough comparison of multiple factors in the MCA between *Dusp5* KO and wild-type (WT) rats. This comprehensive analysis encompassed the intrinsic structural characteristics, myogenic reactivity across a broad range of perfusion pressures (ranging from 40 to 180 mmHg), evaluation of myogenic tone, and assessment of passive mechanical properties.

Materials and methods

Animals

All experiments were conducted on 9- to 12-week-old male WT (FHH.1$^{BN-(D1Rat09-D1Rat225)/Mcwi}$) and *Dusp5* KO (FHH-Chr 1^{BN}-*Dusp5*^{em1Mcwi}) rats that we previously generated and robustly validated [11, 12, 23, 40]. The rats were accommodated in the animal facility at the University of Mississippi Medical Center (UMMC), exposed to a 12-h light–dark cycle with unrestricted access to a standard diet (Teklad rodent diet 8604, Envigo, Indianapolis, IN) and ad libitum water. All procedures conducted in this study were approved by the Institutional Animal Care and Use Committee at UMMC and were meticulously designed and executed in full compliance with the

guidelines established by the American Association for the Accreditation of Laboratory Animal Care.

Assessment of MCA intrinsic structural features

Sample preparation

Samples of the MCA were prepared in accordance with protocols that had been previously published [43]. Briefly, rats were perfused with 10% neutral-buffered formalin (Sigma-Aldrich, St. Louis, MO) intracardially at 100 mmHg after being anesthetized with 2% isoflurane. The brains were retrieved and immersed in 10% formalin for a duration of 2 days for fixation. An approximately 5 mm^3 rectangular piece of brain tissue containing the M1 and M2 segments of the MCA was carefully dissected and embedded with paraffin. Serial cross-sections with a thickness of 3 µm were obtained, encompassing the initial 1 to 2 mm of the M2 segment of the MCA. This segment of the MCA exhibits a consistently cylindrical shape, characterized by vessels with a uniform cylindrical morphology. A systematic random sampling approach was utilized for stereological analysis. This involved the random selection of the first section from among the initial 10 sections, followed by the inclusion of every 10th section thereafter. Four to six sections were evaluated in each animal in this study.

Assessment of VSMC content in the MCA

Evaluation of VSMC content in the MCA wall was conducted through immunofluorescent staining with α-smooth muscle actin (α-SMA) antibody following our published protocol [43]. The formalin-fixed and paraffin-embedded MCA sections underwent deparaffinization using xylene. Subsequently, xylene was removed, and the sections were rehydrated with 100%, 95%, and 70% ethanol, and tap water. After antigen retrieval with proteinase K (S3020, Agilent, Santa Clara, CA), the sections were blocked using Protein Block Serum-Free Blocking (X0909, Agilent, Santa Clara) and incubated with a primary antibody targeting mouse α-SMA (1:300, A5228, Sigma-Aldrich), followed by a secondary antibody, goat anti-mouse (1:1000, A21424, Thermo Fisher Scientific). An anti-fade mounting medium with DAPI (H-1200, Vector Laboratories, Burlingame, CA) was applied, followed by the placement of coverslips. Images were obtained with a Nikon C2 laser scanning confocal system on an Eclipse Ti2 inverted microscope (Nikon, Melville, NY) using a 60X oil immersion objective lens and applying a 3X digital zoom, resulting in a total magnification of 3200X. With a z-step of 1.15 µm, a series of optical sections were captured, and a z-projection was created using three images. The evaluation of α-SMA expression involved comparing fluorescence average intensities per cross-sectional area (CSA) using NIS-Elements Imaging Software 4.6. Furthermore, VSMC counts were manually conducted by visually observing the distinct intercellular spaces between each cell relative to the CSA.

Assessment of collagen content in the MCA

Evaluation of collagen content within the MCA wall involved the use of Masson's trichrome staining, and images were captured using a Nikon Eclipse 55i microscope and a DS-FiL 1 color camera. Collagen quantification within the media and adventitial layers of the MCA wall was achieved by comparing the average intensities of the blue staining with NIS-Elements Imaging Software 4.6.

Assessment of elastin content in the MCA

Evaluation of elastin content in the MCA wall relied on the observation that a linear relationship exists between autofluorescence intensity and elastin content, [44, 45] following a protocol we previously published [43]. Briefly, freshly isolated M2 segments of MCA were fixed with 4% paraformaldehyde at 100 mmHg at 37 °C for 1 h after being cannulated onto glass pipettes in a pressure myograph chamber (Living System Instrumentation, Burlington, VT) and equilibrated in calcium-free physiological salt solution (PSS_{0Ca}). Non-elastin components were removed by incubating with 0.1 M sodium hydroxide at 75 °C for 1 h [43, 44]. Following the removal from the pressure myograph, the vessels were placed onto slides containing a silicon spacer (500 µm depth, 13 mm diameter; Grace Bio Labs, Bend, Oregon) and immersed in VECTASHIELD anti-fade mounting medium (H-1000, Vector Laboratories). Elastin autofluorescence was compared based on the mean autofluorescence intensities per view, which were measured using NIS-Elements Imaging Software 4.6. These measurements were taken from images

of multiple optical sections captured at wavelengths of excitation/emission 488/500–560 nm, utilizing a Nikon C2 laser scanning confocal system on an Eclipse Ti2 inverted microscope with a total magnification of 3200X, as described above. Furthermore, comparisons were made for the thickness of the internal elastic lamina (IEL), the number of fenestrae, and the fenestrae area [44, 46, 47].

Pressure myography

Isolation and preparation of MCA

The MCAs were isolated and prepared following the protocol we had previously documented [2, 6, 48, 49]. In brief, M2 segments of the MCA with an inner diameter (ID) ranging from 150 to 200 µm were meticulously dissected from brain tissues obtained from animals euthanized using 4% isoflurane. The dissected segments were then placed in ice-cold PSS_{0Ca} containing (in mM; pH 7.4): 119 NaCl, 4.7 KCl, 1.17 $MgSO_4$, 18 $NaHCO_3$, 5 HEPES, 1.18 NaH_2PO_4, 10 glucose, and 0.03 EDTA [6, 28, 50].

Assessment of myogenic reactivity of MCA

The impact of *Dusp5* KO on the myogenic response, myogenic tone, and mechanical properties of the MCA was assessed following our published protocol [12, 43]. Briefly, the M2 segments of the MCA dissected and kept in ice-cold PSS_{0Ca} were mounted onto glass pipettes in a single vessel pressure myography chamber (Living System Instrumentation, Burlington, VT) that was filled with calcium-containing physiological salt solution (PSS_{Ca} = PSS_{0Ca} − EDTA + 1.6 mM $CaCl_2$, pH7.4). The chamber was connected to an IMT-2 inverted microscope (Olympus, Center Valley, PA) equipped with a digital camera (AmScope, Irvine, CA). The pH of the PSS_{Ca} was adjusted to 7.4 and maintained at 37 °C using a temperature controller (Living System Instrumentation). The solution was oxygenated with a gas mixture containing 21% O_2, 5% CO_2, and 74% N_2. Intraluminal pressure was regulated via a pressure servo controller (Living System Instrumentation).

The MCAs were pressurized to 40 mmHg for 30 min to allow the development of an equilibration phase with a spontaneous tone. The myogenic response was assessed by comparing the IDs of the vessels in response to intraluminal pressures ranging from 40 to 180 mmHg, in increments of 20 mmHg. After these experiments, the MCAs were washed with PSS_{0Ca} for six to eight times at 5 mmHg. The IDs and outer diameters were recorded.

Assessment of mechanical properties of MCA

In the formulas used in the present study, ID_{0Ca} and OD_{0Ca} represent the ID and OD measured at a specific intraluminal pressure in PSS_{0Ca}, respectively; ID_{Ca} represents the ID measured at the same pressure in PSS_{Ca}; and $ID_{0Ca5mmHg}$ represents the ID measured at 5 mmHg in PSS_{0Ca}. Myogenic response was evaluated by comparing inner diameters across perfusion pressures from 40 to 180 mmHg, presented as a percentage relative to the inner diameter at 40 mmHg. Myogenic tone was calculated at each transmural pressure using the previously described formula [44, 51]:

$$\text{Myogenictone}(\%) = \left[\text{ID}_{0\text{Ca}} - \text{ID}_{\text{Ca}}\right)/\text{ID}_{0\text{Ca}}\right] \times 100.$$

Wall thickness, CSA, and wall-to-lumen ratio were determined using the following formulas:

$$\text{Wallthickness}(\mu\text{m}) = \left(\text{OD}_{0\text{Ca}} - \text{ID}_{0\text{Ca}}\right)/2$$

$$\text{CSA}\left(\mu\text{m}^2\right) = (\pi/4)\text{X}\left(\text{OD}_{0\text{Ca}}^2 - \text{ID}_{0\text{Ca}}^2\right)$$

$$\text{Wall/lumenratio} = \text{Wallthickness}/\text{ID}_{0\text{Ca}}$$

Distensibility, regarded as an essential indicator of vascular compliance, represents the ability of the artery to function as a buffer. Distensibility plays a crucial role in determining stress on the vessel wall, and a reduction in distensibility could elevate the risk of damage to the arterial wall [12, 43]. Incremental distensibility refers to the percentage of change in the ID_{0Ca} (ΔID_{0Ca}) of the blood vessel for every 1 mmHg change in pressure (ΔP). The following equations were applied in the present study:

$$\text{Distensibility}(\%) = \left(\text{ID}_{0\text{Ca}} - \text{ID}_{0\text{Ca5mmHg}}\right)/\text{ID}_{0\text{Ca5mmHg}} \times 100$$

$$\text{Incrementaldistensibility}(\%/\text{mmHg}) = \Delta\text{ID}_{0\text{Ca}}/\left(\text{ID}_{0\text{Ca}} \times \Delta\text{P}\right) \times 100$$

Circumferential wall strain refers to the deformation or stretching of a blood vessel, along its circumference in response to changes in pressure.

Circumferential wall stress refers to the mechanical force per unit area acting on the circumferential of a blood vessel. These parameters are important in understanding the mechanical behavior of blood vessels and their ability to adapt to changes in blood flow and pressure.

$$\text{Circumferential wall strain}(\varepsilon) = \left(\text{ID}_{0\text{Ca}} - \text{ID}_{0\text{Ca5mmHg}}\right)/\text{ID}_{0\text{Ca5mmHg}}$$

$$\text{Circumferential wall stress}(\sigma) = \left(\text{P} \times \text{ID}_{0\text{Ca}}\right)/2\text{WT}$$

Elastic modulus ($E = \sigma / \varepsilon$) is an important property of evaluation of arterial stiffness [46]. The slopes (β-values) of an exponential model with least-squares analysis of the elastic modulus ($\sigma = \sigma_{orig} e^{\beta\varepsilon}$; σ_{orig} is σ at 5 mmHg) were compared to determine the arterial stiffness. An increased β value (a higher value of elastic modulus) indicated a stiffer vessel.

Statistical analyses

All data are represented as mean values accompanied by the standard error of the mean (SEM). We employed a two-way analysis of variance (ANOVA) for repeated measures, followed by a Holm-Sidak post hoc test, to assess significant differences between *Dusp5* KO and WT rats in the pressure myograph studies. For the corresponding values of immunohistochemistry and β-values between the two groups, an unpaired *t*-test with Welch's correction was utilized to determine significance. All statistical analyses were conducted using GraphPad Prism 6 software (GraphPad Software, Inc.), with statistical significance defined as $p < 0.05$.

Results

Impacts of knockout of Dusp5 on VSMC content in the MCA

Immunofluorescence staining with an α-SMA antibody showed no significant difference in the number of VSMCs across the cross-section of the MCA wall between *Dusp5* KO ($9965.46 \pm 465.63/mm^2$) and WT ($10{,}884.07 \pm 324.66/mm^2$) rats (Fig. 1).

Impacts of knockout of Dusp5 on collagen content in the MCA

The differences in the collagen content between *Dusp5* and WT rats, determined by Masson's trichrome staining, are depicted in Fig. 2. Our results indicate no significant difference in the average blue intensity, which represents the collagen-specific methyl blue, within the tunica media and tunica adventitia of the MCA between *Dusp5* KO and WT rats.

Impacts of knockout of Dusp5 on elastin content in the MCA

The effects of knockout of *Dusp5* on elastin content in the MCA are presented in Fig. 3. We first verified the absence of the external elastic lamina in MCA in both *Dusp5* KO and WT rats [43, 52]. The autofluorescence intensity was notably higher in the MCA of *Dusp5* KO (953.76 ± 10.03 a.u.) compared to WT control rats (737.31 ± 64.88 a.u.) (Fig. 3A). The thickness of the IEL was significantly increased in the MCA of *Dusp5* KO (2.33 ± 0.02 μm) compared to WT control rats (1.85 ± 0.03 μm) (Fig. 3B). Additionally, *Dusp5* KO MCA displayed a reduced number of fenestrations and smaller fenestrae areas compared to WT controls (Fig. 3C–F). These findings collectively indicate significant differences in the elastin composition and structure within the MCA wall between *Dusp5* and WT rats.

Impacts of knockout of Dusp5 on myogenic reactivity and tone in the MCA

The baseline IDs of the MCA in *Dusp5* KO (196.79 ± 8.15 μm) and WT (205.88 ± 4.45 μm) rats were comparable. In response to increased perfusion pressure from 40 to 100, 140, and 180 mmHg, the MCA in *Dusp5* KO rats constricted to $86.89 \pm 0.02\%$, $78.55 \pm 2.02\%$, and $81.83 \pm 2.35\%$, respectively (Fig. 4A). These constriction responses were significantly enhanced compared to those in WT rats ($91.87 \pm 1.16\%$, $88.32 \pm 2.10\%$, and $90.68 \pm 3.10\%$ at the same pressures), demonstrating a more dynamic and pronounced vascular response to pressure changes. On the other hand, the passive diameters

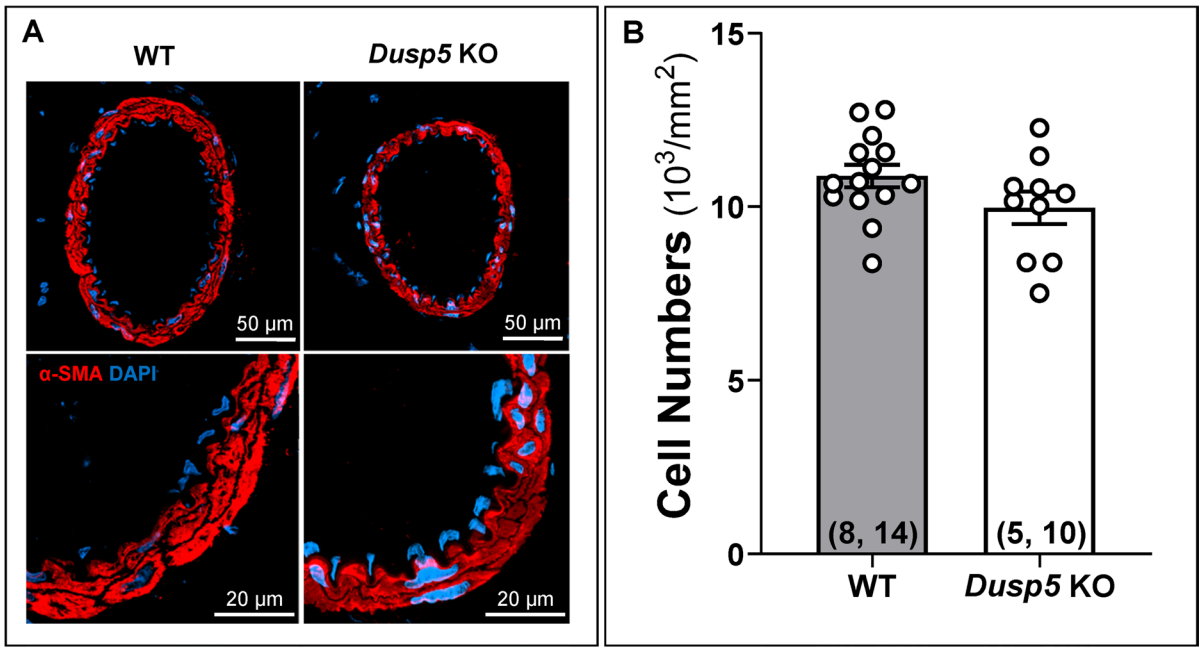

Fig. 1 Impacts of *Dusp5* knockout (KO) on vascular smooth muscle cell (VSMC) content in the middle cerebral artery (MCA). **A** Representative images illustrating the expression of α-SMA in the MCA wall of male *Dusp5* KO and wild-type (WT) rats. **B** Comparison of VSMC numbers across the cross-sectional area of the MCA wall in male *Dusp5* KO and WT rats. Mean values ± SEM are presented, with the numbers in parentheses indicating the number of rats and vessels studied per group (n = # rats, # vessels)

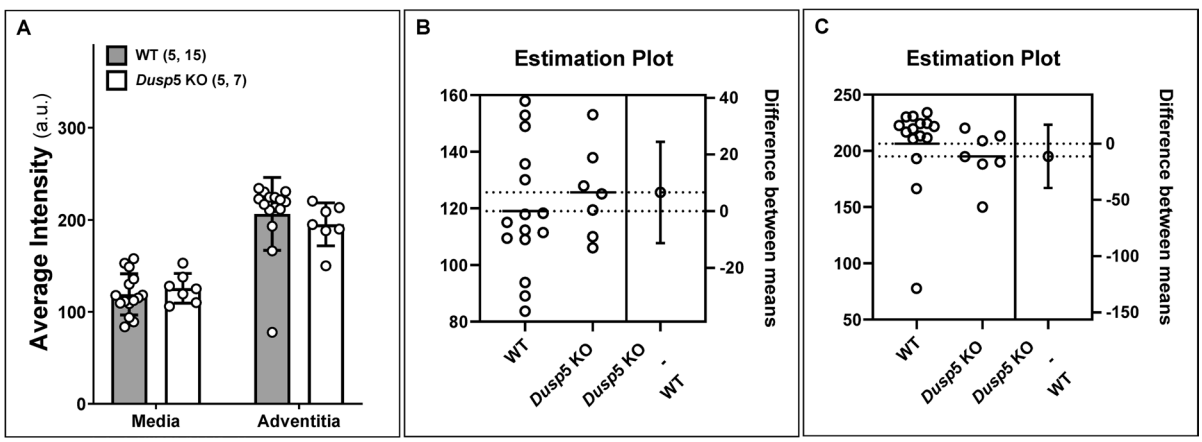

Fig. 2 Impacts of *Dusp5* knockout (KO) on collagen content in the middle cerebral artery (MCA). **A** The average artificial unit (a.u.) of fluorescence intensity was compared across the cross-sectional area in the tunica media and adventitia of the MCA in male *Dusp5* KO and wild-type (WT) rats. Estimation plots depicting fluorescence intensity in the media **(B)** and adventitia **(C)** of the MCA in *Dusp5* KO and WT rats are presented. Mean values ± SEM are provided, with the numbers in parentheses indicating the number of rats and vessels studied per group (n = # rats, # vessels)

(IDs_{0Ca}) of the MCA were similar in *Dusp5* KO and WT rats at perfusion pressure ranging from 40 to 180 mmHg (Fig. 4B). *Dusp5* KO rats also exhibited an enhanced myogenic tone under perfusion pressures ranging from 40 to 180 mmHg (Fig. 4C).

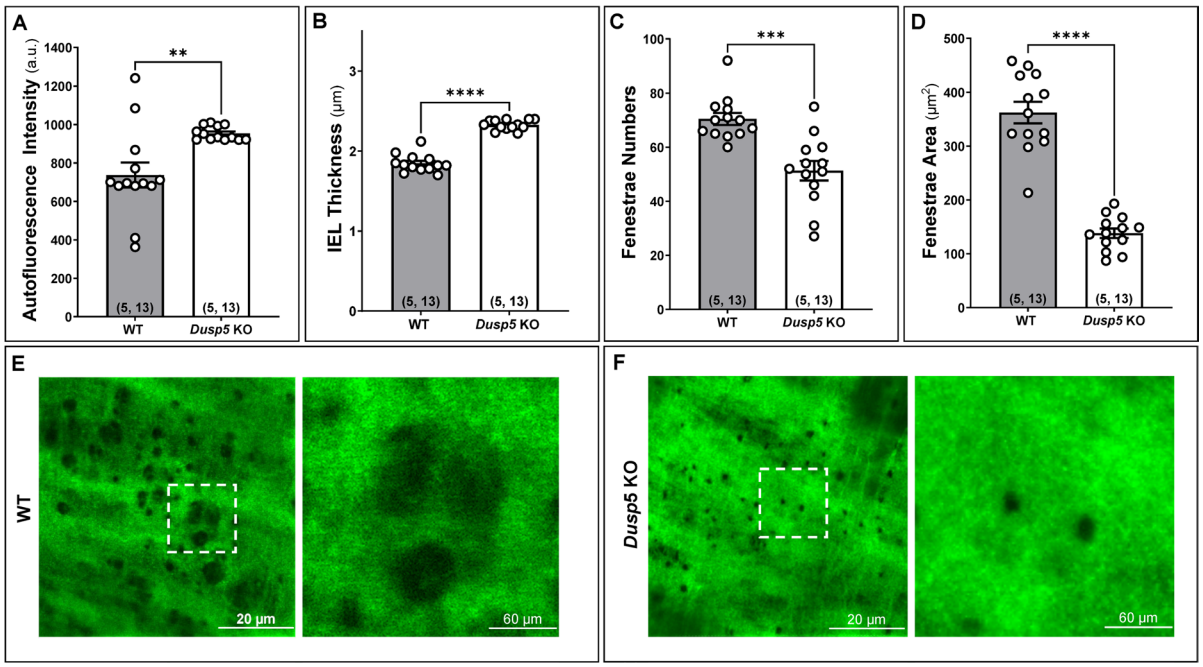

Fig. 3 Impacts of *Dusp5* knockout (KO) on elastin content in the middle cerebral artery (MCA). In the MCA of male *Dusp5* KO and wild-type (WT) rats, we compared **A** the average artificial unit (a.u.) of the autofluorescence intensity in the internal elastic lamina (IEL), **B** the IEL thickness, **C** the fenestrae numbers in the IEL, and **D** the fenestrae areas in the IEL. **E, F** Representative images of the elastin autofluorescence in the IEL detected by confocal microscopy. Mean values ± SEM are presented, with the numbers in parentheses indicating the number of rats and vessels studied per group (n = # rats, # vessels). One, two, three, and four asterisks (*) indicate $p < 0.05$, 0.01, 0.001, and 0.0001, respectively, from the corresponding values in *Dusp5* KO versus WT rats

Impacts of knockout of Dusp5 on mechanical properties of the MCA

The wall thickness (Fig. 5A), wall-to-lumen ratio (Fig. 5B), and CSA (Fig. 5C) of the MCA in *Dusp*5 KO rats did not show significant changes compared to wild-WT rats across perfusion pressure ranging from 40 to 180 mmHg. Moreover, the MCA in *Dusp*5 KO rats exhibits comparable distensibility (Fig. 6A), incremental distensibility (Fig. 6B), as well as circumferential wall stress (Fig. 7A), elastic modulus (Fig. 7B), and β-values (Fig. 7C). These results suggest that DUSP5 is unlikely to contribute to significant changes in MCA vascular remodeling, distensibility, and stiffness under physiological conditions.

Discussion

Vascular aging involves structural and functional changes in blood vessels over time, significantly impacting hemodynamics—the dynamic blood flow within the circulatory system. Aging brings about a range of vascular alterations, including changes in intrinsic vessel structure, compliance, remodeling, arterial stiffness, and endothelial function. These modifications collectively influence hemodynamic patterns, affecting the dynamic flow of blood. This, in turn, heightens the risk for various vascular diseases [1]. Importantly, emerging research suggests a connection between vascular aging and neurodegenerative conditions like AD/ADRD [53]. The compromised blood flow to the brain due to vascular aging may play a role in the development and progression of cognitive decline and neurodegeneration [3, 34]. Understanding the intricate relationship between vascular aging, hemodynamics, and neurological health

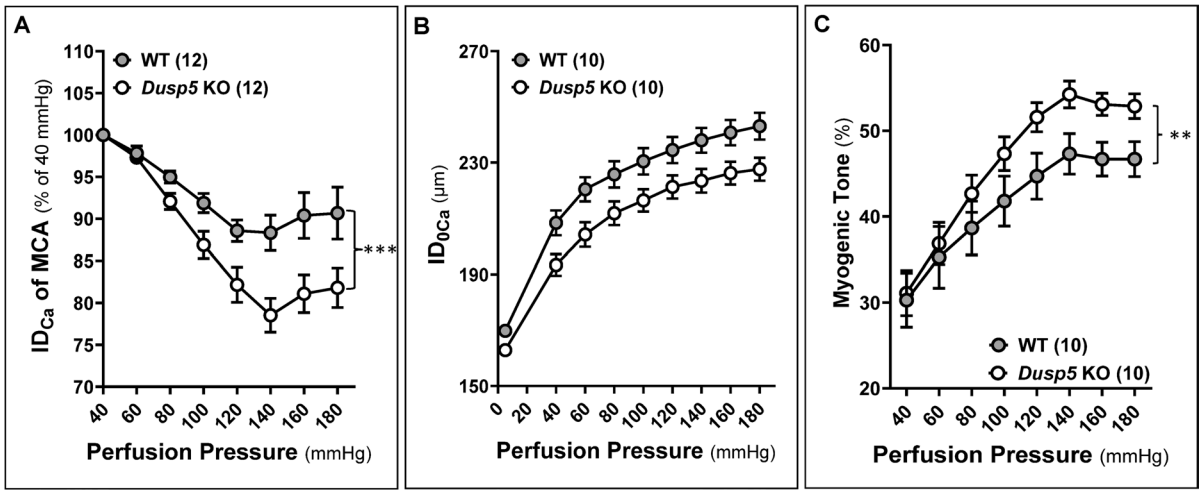

Fig. 4 Impacts of *Dusp5* knockout (KO) on myogenic reactivity and tone in the middle cerebral artery (MCA). **A** Comparison of the myogenic response of MCA of *Dusp5* KO and wild-type (WT) rats in response to an elevation in perfusion pressure ranging from 40 to 180 mmHg. **B** Comparison of the passive diameters (IDs_{0Ca}) of the MCA in *Dusp5* KO and WT rats at perfusion pressure ranging from 40 to 180 mmHg. **C** Comparison of the myogenic tone of MCA of *Dusp5* KO and WT rats across perfusion pressure ranging from 40 to 180 mmHg. Mean values ± SEM are presented. Numbers in parentheses indicate the number of rats studied per group. One, two, three, and four asterisks (*) indicate adjust $p < 0.05$, 0.01, 0.001, and 0.0001, respectively, from the corresponding values in *Dusp5* KO versus WT rats after the post hoc test

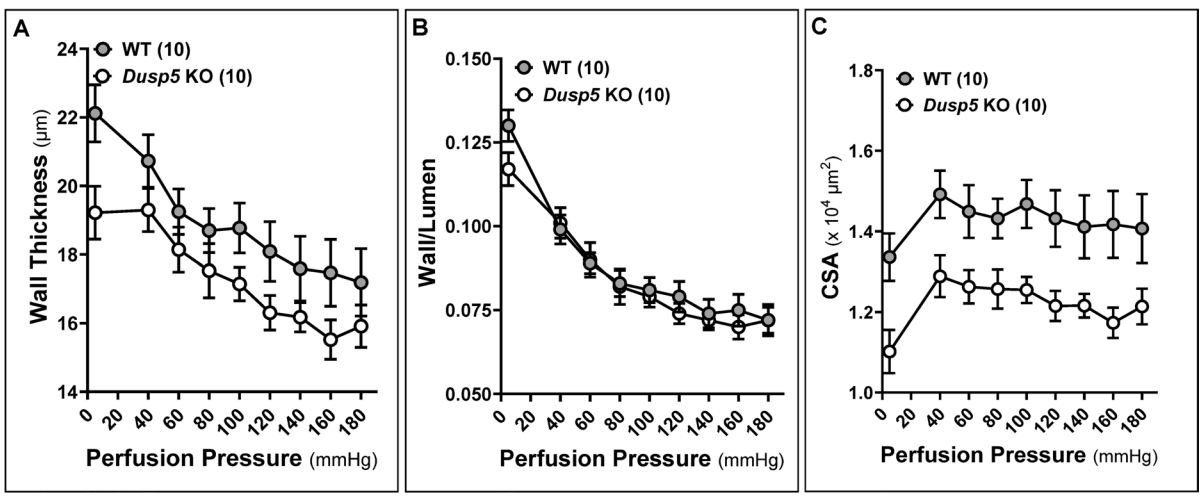

Fig. 5 Impacts of *Dusp5* knockout (KO) on wall thickness, wall-to-lumen ratio, and cross-sectional area (CSA) of the middle cerebral artery (MCA). **A** Comparison of the wall thickness of MCA of *Dusp5* KO and wild-type (WT) rats across perfusion pressure ranging from 40 to 180 mmHg. **B** Comparison of the wall-to-lumen ratio of MCA of *Dusp5* KO and WT rats. **C** Comparison of the CSA of MCA of *Dusp5* KO and WT rats. Numbers in parentheses indicate the number of rats studied per group. One, two, three, and four asterisks (*) indicate adjust $p < 0.05$, 0.01, 0.001, and 0.0001, respectively, from the corresponding values in *Dusp5* KO versus WT rats after the post hoc test

is crucial for developing targeted interventions to mitigate the risks associated with aging and promote overall vascular and cognitive well-being.

We recently reported that KO of *Dusp5* results in improved cerebral and renal hemodynamics and cognitive function [11, 12, 23, 40]. This enhancement

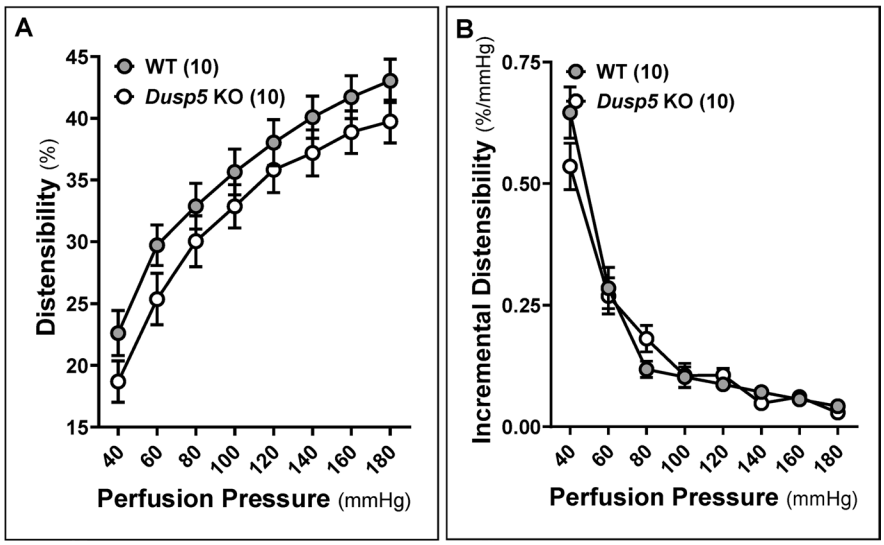

Fig. 6 Impacts of *Dusp5* knockout (KO) on distensibility and incremental distensibility of the middle cerebral artery (MCA). **A** Comparison of distensibility of MCA of *Dusp5* KO and wild-type (WT) rats across perfusion pressure ranging from 40 to 180 mmHg. **B** Comparison of incremental distensibility of MCA of *Dusp5* KO and WT rats. The numbers in parentheses indicate the number of rats studied per group. One, two, three, and four asterisks (*) indicate adjust $p < 0.05$, 0.01, 0.001, and 0.0001, respectively, from the corresponding values in *Dusp5* KO versus WT rats after the post hoc test

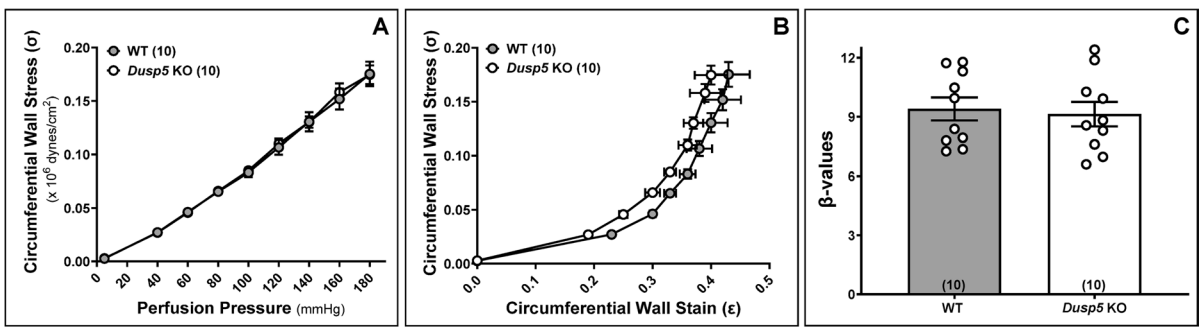

Fig. 7 Impacts of *Dusp5* knockout (KO) on circumferential wall stress, elastic modulus (stress/strain), and β stiffness of the middle cerebral artery (MCA). **A** Comparison of circumferential wall stress of MCA of *Dusp5* KO and wild-type (WT) rats across perfusion pressure ranging from 40 to 180 mmHg. **B** Comparison of elastic modulus (stress/strain) in MCA of *Dusp5* KO and WT rats. **C** Comparison of the slopes of the elastic modulus curves (β values) in the MCA of *Dusp5* KO and WT rats. Numbers in parentheses indicate the number of rats studied per group. 1 mmHg = 1,334 dynes/cm^2

is associated with elevated levels of pPKC and pERK1/2 in the brain and kidneys. Notably, *Dusp*5 KO also influences the passive mechanical properties of cerebral and renal arterioles, manifesting as increased myogenic tone, enhanced distensibility, greater compliance, and reduced stiffness [12]. These modifications in vascular properties are observed in both MCAs and PAs, coinciding with increased CBF autoregulation on the surface and in the deep cortex of the brain. While our previous studies concentrated on the PAs, the present study evaluates the impacts of *Dusp*5 KO on the structural and mechanical characteristics of the MCAs.

Intrinsic structural shifts pertain to the physical composition of vessels. In the arterial wall, the three primary layers are composed of the intima, media, and adventitia. The intima is comprised of the IEL and endothelial cells. Progressing outward, the media

is characterized by elastin organized into sheets (lamellae), along with collagen, VSMCs, and the extracellular matrix. The outermost layer is formed by the adventitia, which contributes to vascular stiffness and compliance with longitudinally arranged collagen along the vessel wall. This organized structure ensures the stability, elasticity, and overall functionality of the blood vessels [43]. By comparing the VSMC, elastin, and collagen contents in the MCA, our study revealed no significant difference in VSMC and collagen contents between KO and WT rats. However, KO of *Dusp5* led to notable changes in elastin content and structure in the MCA, with higher autofluorescence intensity, increased IEL thickness, and reduced elastin fenestrations compared to WT controls.

VSMCs play a pivotal role in maintaining the structural integrity of blood vessels and dynamically regulating changes in diameter in response to various stimuli [2, 54]. Despite the unaffected numbers of VSMCs in the context of *Dusp5* KO, the MCA exhibits an enhanced myogenic response and increased contractility of cerebral VSMCs [11, 12, 40]. This suggests a potential linkage to the enzymatic function of DUSP5, implicating its role in modulating vascular dynamics and contractile properties. DUSP5 is a multifaceted regulator of the MAPK signaling pathway with broad implications in various cellular processes, vascular regulation, hypertension, renal injury, cognitive function, and cancer biology [13]. As an enzyme, DUSP5 exerts a negative regulatory influence on ERK1/2 in association with PKC. This interaction potentially enhances calcium influx in VSMCs and facilitates vasoconstriction in *Dusp5* KO animals, thereby influencing vascular dynamics [41].

Similar to observations in PAs, the myogenic tone in the MCA was enhanced in *Dusp5* KO rats. Nevertheless, various passive mechanical properties of the MCA, encompassing parameters such as passive IDs, wall thickness, wall-to-lumen ratio, CSA, distensibility, incremental distensibility, circumferential wall stress, elastic modulus, and β stiffness, did not display significant alterations in the context of this study. The aforementioned parameters collectively assess vascular remodeling, compliance, distensibility, and stiffness. Our results demonstrated that KO of *Dusp5* did not affect MCA vascular remodeling under healthy conditions. Collagen is a crucial structural component in the arterial wall, providing reinforcement and constituting the primary non-distensible element and significantly contributing to vascular stiffness and compliance. The result showed that the collagen content is comparable between *Dusp5* KO and WT rats, consistent with similar distensibility and stiffness between these two strains of animals. Elastin plays a crucial role in stabilizing the structure of arteries. When blood pressure increases, elastic fibers in the MCA wall stretch, which can trigger the myogenic response. With a thicker IEL in MCA of *Dusp5* KO and an enhanced myogenic response, the increased tendency to constrict (in response to pressure or stretch) contributes to a higher myogenic tone. The observed differences in elastin fenestrations and IEL thickness may contribute to variations in the mechanical properties of MCA, potentially impacting its myogenic response and tone. Given that CBF autoregulation is mainly mediated by myogenic response and poor CBF autoregulation has been associated with cognitive decline [55], it underscores the potential impact and significance of elastin in maintaining vascular health and cognitive function.

In conclusion, our study delves into the consequences of *Dusp5* KO on the structural and mechanical characteristics of the MCA. Remarkably, we observe substantial increases in the thickness of the IEL and changes in elastin structure within the MCA of *Dusp5* KO rats. Intriguingly, these alterations manifest without corresponding adjustments in VSMC numbers or collagen content in the vascular wall. The current understanding suggests that these elastic modifications, coupled with the enzymatic activity of DUSP5, likely contribute significantly to the enhanced myogenic response and tone in the MCA, as well as the reported improvements in CBF autoregulation and cognition in *Dusp5* KO animals. Although our study exclusively focuses on young, healthy male animals, the potential impact of *Dusp5* KO on aging vessels and vascular function-related diseases warrants further investigation using aged animal models and the potential therapeutic translation of DUSP5 activators or inhibitors.

Our study has highlighted the significant role of *Dusp5* knockout in altering the structural and mechanical characteristics of the MCA, particularly noting the increases in the thickness of the IEL and changes in elastin structure. While these findings provide valuable insights, with limitations that are only studied in young, healthy male animals, a more

detailed expanded exploration of the underlying mechanisms by which *Dusp*5 knockout influences vascular properties could be beneficial. Understanding these mechanisms in greater depth may open avenues for translating these findings into therapeutic strategies or preventive measures for vascular aging and related neurodegenerative diseases, such as AD/ADRD.

Author contribution HZ and FF conceived and designed research; HZ, CT, JB, YL, XF, and JRJ performed experiments; CT, HZ, JB, TJL, SB, AS, and FF analyzed data; CT, HZ, JB, RJR, and FF interpreted results; CT, HZ, JB, and FF prepared figures; CT, JB, HZ, and FF drafted the manuscript; CT, AG, CJ, TJL, SB, AS, SMS, HY, RJR, and FF edited and revised the manuscript; all authors approved the final version of the manuscript.

Funding This study was supported by grants AG079336, AG057842, P20GM104357, and HL138685 from the National Institutes of Health, and TRIBA Faculty Startup Fund from Augusta University.

Data availability The data supporting the findings of this study are available upon reasonable request from the corresponding author.

Declarations

Conflict of interest The authors declare no competing interests.

References

1. Ungvari Z, Tarantini S, Donato AJ, Galvan V, Csiszar A. Mechanisms of vascular aging. Circ Res. 2018;123:849–67. https://doi.org/10.1161/CIRCRESAHA.118.311378.
2. Guo Y, Wang S, Liu Y, Fan L, Booz GW, Roman RJ, Chen Z, Fan F. Accelerated cerebral vascular injury in diabetes is associated with vascular smooth muscle cell dysfunction. Geroscience. 2020;42:547–61. https://doi.org/10.1007/s11357-020-00179-z.
3. Shekhar S, Liu R, Travis OK, Roman RJ, Fan F. Cerebral autoregulation in hypertension and ischemic stroke: A mini review. J Pharm Sci Exp Pharmacol. 2017;2017:21–7.
4. Wang S, Lv W, Zhang H, Liu Y, Li L, Jefferson JR, Guo Y, Li M, Gao W, Fang X, et al. Aging exacerbates impairments of cerebral blood flow autoregulation and cognition in diabetic rats. Geroscience. 2020;42:1387–410. https://doi.org/10.1007/s11357-020-00233-w.
5. Fan F, Ge Y, Lv W, Elliott MR, Muroya Y, Hirata T, Booz GW, Roman RJ. Molecular mechanisms and cell signaling of 20-hydroxyeicosatetraenoic acid in vascular pathophysiology. Front Biosci (Landmark Ed). 2016;21:1427–63.
6. Fan F, Geurts AM, Murphy SR, Pabbidi MR, Jacob HJ, Roman RJ. Impaired myogenic response and autoregulation of cerebral blood flow is rescued in CYP4A1 transgenic Dahl salt-sensitive rat. Am J Physiol Regul Integr Comp Physiol. 2015;308:R379-390. https://doi.org/10.1152/ajpregu.00256.2014.
7. Fan F, Geurts AM, Pabbidi MR, Ge Y, Zhang C, Wang S, Liu Y, Gao W, Guo Y, Li L, et al. A mutation in gamma-adducin impairs autoregulation of renal blood flow and promotes the development of kidney disease. J Am Soc Nephrol. 2020;31:687–700. https://doi.org/10.1681/ASN.2019080784.
8. Fan F, Simino J, Auchus AP, Knopman DS, Boerwinkle E, Fornage M, Mosley TH, Roman RJ. Functional variants in CYP4A11 and CYP4F2 are associated with cognitive impairment and related dementia endophenotypes in the elderly. Paper presented at: The 16th International Winter Eicosanoid Conference. Baltimore; 2016.
9. Bloom SI, Tucker JR, Lim J, Thomas TG, Stoddard GJ, Lesniewski LA, Donato AJ. Aging results in DNA damage and telomere dysfunction that is greater in endothelial versus vascular smooth muscle cells and is exacerbated in atheroprone regions. Geroscience. 2022;44:2741–55. https://doi.org/10.1007/s11357-022-00681-6.
10. Tucsek Z, NoaValcarcel-Ares M, Tarantini S, Yabluchanskiy A, Fulop G, Gautam T, Orock A, Csiszar A, Deak F, Ungvari Z. Hypertension-induced synapse loss and impairment in synaptic plasticity in the mouse hippocampus mimics the aging phenotype: Implications for the pathogenesis of vascular cognitive impairment. Geroscience. 2017;39:385–406. https://doi.org/10.1007/s11357-017-9981-y.
11. Fan F, Geurts AM, Pabbidi MR, Smith SV, Harder DR, Jacob H, Roman RJ. Zinc-finger nuclease knockout of dual-specificity protein phosphatase-5 enhances the myogenic response and autoregulation of cerebral blood flow in FHH.1BN rats. PLoS One. 2014;9:e112878. https://doi.org/10.1371/journal.pone.0112878.
12. Zhang H, Zhang C, Liu Y, Gao W, Wang S, Fang X, Guo Y, Li M, Liu R, Roman RJ, et al. Influence of dual-specificity protein phosphatase 5 on mechanical properties of rat cerebral and renal arterioles. Physiol Rep. 2020;8:e14345. https://doi.org/10.14814/phy2.14345.
13. Kucharska A, Rushworth LK, Staples C, Morrice NA, Keyse SM. Regulation of the inducible nuclear dual-specificity phosphatase DUSP5 by ERK MAPK. Cell Signal. 2009;21:1794–805. https://doi.org/10.1016/j.cellsig.2009.07.015.
14. Mandl M, Slack DN, Keyse SM. Specific inactivation and nuclear anchoring of extracellular signal-regulated kinase 2 by the inducible dual-specificity protein phosphatase DUSP5. Mol Cell Biol. 2005;25:1830–45. https://doi.org/10.1128/MCB.25.5.1830-1845.2005.
15. Mebratu Y, Tesfaigzi Y. How ERK1/2 activation controls cell proliferation and cell death: Is subcellular localization the answer? Cell Cycle. 2009;8:1168–75. https://doi.org/10.4161/cc.8.8.8147.
16. Jo HJ, Yang JW, Park JH, Choi ES, Lim CS, Lee S, Han CY. Endoplasmic reticulum stress increases DUSP5 expression via PERK-CHOP pathway, leading to hepatocyte death. Int J Mol Sci. 2019;20(18):4369. https://doi.org/10.3390/ijms20184369.

17. Liang M, Li Y, Zhang K, Zhu Y, Liang J, Liu M, Zhang S, Chen D, Liang H, Liang L, et al. Host factor DUSP5 potently inhibits dengue virus infection by modulating cytoskeleton rearrangement. Antiviral Res. 2023;215:105622. https://doi.org/10.1016/j.antiviral.2023.105622.
18. Ferguson BS, Wennersten SA, Demos-Davies KM, Rubino M, Robinson EL, Cavasin MA, Stratton MS, Kidger AM, Hu T, Keyse SM, et al. DUSP5-mediated inhibition of smooth muscle cell proliferation suppresses pulmonary hypertension and right ventricular hypertrophy. Am J Physiol Heart Circ Physiol. 2021;321:H382-h389. https://doi.org/10.1152/ajpheart.00115.2021.
19. Wu Z, Xu L, He Y, Xu K, Chen Z, Moqbel SAA, Ma C, Jiang L, Ran J, Wu L, et al. DUSP5 suppresses interleukin-1β-induced chondrocyte inflammation and ameliorates osteoarthritis in rats. Aging (Albany NY). 2020;12:26029–46. https://doi.org/10.18632/aging.202252.
20. Mengozzi M, Cervellini I, Villa P, Erbayraktar Z, Gökmen N, Yilmaz O, Erbayraktar S, Manohasandra M, Van Hummelen P, Vandenabeele P, et al. Erythropoietin-induced changes in brain gene expression reveal induction of synaptic plasticity genes in experimental stroke. Proc Natl Acad Sci U S A. 2012;109:9617–22. https://doi.org/10.1073/pnas.1200554109.
21 Wang J, Cao B, Han D, Sun M, Feng J. Long non-coding RNA H19 induces cerebral ischemia reperfusion injury via activation of autophagy. Aging Dis. 2017;8:71–84. https://doi.org/10.14336/ad.2016.0530.
22. Moon SJ, Lim MA, Park JS, Byun JK, Kim SM, Park MK, Kim EK, Moon YM, Min JK, Ahn SM, et al. Dual-specificity phosphatase 5 attenuates autoimmune arthritis in mice via reciprocal regulation of the Th17/Treg cell balance and inhibition of osteoclastogenesis. Arthritis Rheumatol. 2014;66:3083–95. https://doi.org/10.1002/art.38787.
23. Zhang C, He X, Murphy SR, Zhang H, Wang S, Ge Y, Gao W, Williams JM, Geurts AM, Roman RJ, et al. Knockout of dual-specificity protein phosphatase 5 protects against hypertension-induced renal injury. J Pharmacol Exp Ther. 2019;370:206–17. https://doi.org/10.1124/jpet.119.258954.
24. An N, Bassil K, Al Jowf GI, Steinbusch HWM, Rothermel M, de Nijs L, Rutten BPF. Dual-specificity phosphatases in mental and neurological disorders. Prog Neurobiol. 2021;198:101906. https://doi.org/10.1016/j.pneurobio.2020.101906.
25. Hevroni D, Rattner A, Bundman M, Lederfein D, Gabarah A, Mangelus M, Silverman MA, Kedar H, Naor C, Kornuc M, et al. Hippocampal plasticity involves extensive gene induction and multiple cellular mechanisms. J Mol Neurosci. 1998;10:75–98. https://doi.org/10.1007/bf02737120.
26. Grupe A, Li Y, Rowland C, Nowotny P, Hinrichs AL, Smemo S, Kauwe JS, Maxwell TJ, Cherny S, Doil L, et al. A scan of chromosome 10 identifies a novel locus showing strong association with late-onset Alzheimer disease. Am J Hum Genet. 2006;78:78–88. https://doi.org/10.1086/498851.
27. Webster JA, Gibbs JR, Clarke J, Ray M, Zhang W, Holmans P, Rohrer K, Zhao A, Marlowe L, Kaleem M, et al. Genetic control of human brain transcript expression in Alzheimer disease. Am J Hum Genet. 2009;84:445–58. https://doi.org/10.1016/j.ajhg.2009.03.011.
28. Fang X, Tang C, Zhang H, Border JJ, Liu Y, Shin SM, Yu H, Roman RJ, Fan F. Longitudinal characterization of cerebral hemodynamics in the TgF344-AD rat model of Alzheimer's disease. Geroscience. 2023. https://doi.org/10.1007/s11357-023-00773-x.
29. Gonzalez-Fernandez E, Liu Y, Auchus Alexander P, Fan F, Roman R. Vascular contributions to cognitive impairment and dementia: The emerging role of 20-HETE. Clin Sci. 2021;135:1929–44. https://doi.org/10.1042/CS20201033.
30. Fang X, Zhang J, Roman RJ, Fan F. From 1901 to 2022, how far are we from truly understanding the pathogenesis of age-related dementia? GeroScience. 2022;44:1879–83. https://doi.org/10.1007/s11357-022-00591-7.
31. Fang X, Crumpler RF, Thomas KN, Mazique JN, Roman RJ, Fan F. Contribution of cerebral microvascular mechanisms to age-related cognitive impairment and dementia. Physiol Int. 2022. https://doi.org/10.1556/2060.2022.00020.
32. Fan F, Roman RJ. Reversal of cerebral hypoperfusion: A novel therapeutic target for the treatment of AD/ADRD? Geroscience. 2021;43:1065–7. https://doi.org/10.1007/s11357-021-00357-7.
33 Crumpler R, Roman RJ, Fan F. Capillary stalling: A mechanism of decreased cerebral blood flow in AD/ADRD. J Exp Neurol. 2021;2:149–53. https://doi.org/10.33696/neurol.2.048.
34. Shekhar S, Wang S, Mims PN, Gonzalez-Fernandez E, Zhang C, He X, Liu CY, Lv W, Wang Y, Huang J, et al. Impaired cerebral autoregulation-A common neurovascular pathway in diabetes may play a critical role in diabetes-related Alzheimer's disease. Curr Res Diabetes Obes J. 2017;2:555587.
35. Wang S, Mims PN, Roman RJ, Fan F. Is beta-amyloid accumulation a cause or consequence of Alzheimer's disease? J Alzheimers Parkinsonism Dement. 2016;1(2):007.
36. Zhang H, Roman R, Fan F. Hippocampus is more susceptible to hypoxic injury: Has the Rosetta Stone of regional variation in neurovascular coupling been deciphered? GeroScience. 2021. https://doi.org/10.1007/s11357-021-00449-4.
37. Lipecz A, Miller L, Kovacs I, Czakó C, Csipo T, Baffi J, Csiszar A, Tarantini S, Ungvari Z, Yabluchanskiy A, et al. Microvascular contributions to age-related macular degeneration (AMD): From mechanisms of choriocapillaris aging to novel interventions. Geroscience. 2019;41:813–45. https://doi.org/10.1007/s11357-019-00138-3.
38. Kiss T, Nyúl-Tóth Á, Balasubramanian P, Tarantini S, Ahire C, DelFavero J, Yabluchanskiy A, Csipo T, Farkas E, Wiley G, et al. Single-cell RNA sequencing identifies senescent cerebromicrovascular endothelial cells in the aged mouse brain. Geroscience. 2020;42:429–44. https://doi.org/10.1007/s11357-020-00177-1.
39. Fulop GA, Ahire C, Csipo T, Tarantini S, Kiss T, Balasubramanian P, Yabluchanskiy A, Farkas E, Toth A, Nyúl-Tóth Á, et al. Cerebral venous congestion

promotes blood-brain barrier disruption and neuroinflammation, impairing cognitive function in mice. Geroscience. 2019;41:575–89. https://doi.org/10.1007/s11357-019-00110-1.
40. Zhang H, Border JJ, Fang X, Liu Y, Tang C, Gao W, Wang S, Shin SM, Guo Y, Zhang C, et al. Enhanced cerebral hemodynamics and cognitive function via knockout of dual-specificity protein phosphatase 5. J Pharm Pharmacol Res. 2023;7:49–61. https://doi.org/10.26502/fjppr.070.
41. Wickramasekera NT, Gebremedhin D, Carver KA, Vakeel P, Ramchandran R, Schuett A, Harder DR. Role of dual-specificity protein phosphatase-5 in modulating the myogenic response in rat cerebral arteries. J Appl Physiol. 1985;2013(114):252–61. https://doi.org/10.1152/japplphysiol.01026.2011.
42. Navarro-Orozco D, Sanchez-Manso JC. Neuroanatomy, middle cerebral artery. In: StatPearls [Internet]. Treasure Island (FL): StatPearls Publishing; 2023.
43. Wang S, Zhang H, Liu Y, Li L, Guo Y, Jiao F, Fang X, Jefferson JR, Li M, Gao W, et al. Sex differences in the structure and function of rat middle cerebral arteries. Am J Physiol Heart Circ Physiol. 2020;318:H1219–32. https://doi.org/10.1152/ajpheart.00722.2019.
44. Briones AM, Gonzalez JM, Somoza B, Giraldo J, Daly CJ, Vila E, Gonzalez MC, McGrath JC, Arribas SM. Role of elastin in spontaneously hypertensive rat small mesenteric artery remodelling. J Physiol. 2003;552:185–95. https://doi.org/10.1113/jphysiol.2003.046904.
45. Blomfield J, Farrar JF. The fluorescent properties of maturing arterial elastin. Cardiovasc Res. 1969;3:161–70. https://doi.org/10.1093/cvr/3.2.161.
46. Pourageaud F, Crabos M, Freslon JL. The elastic modulus of conductance coronary arteries from spontaneously hypertensive rats is increased. J Hypertens. 1997;15:1113–21. https://doi.org/10.1097/00004872-199715100-00009.
47. Sandow SL, Gzik DJ, Lee RM. Arterial internal elastic lamina holes: Relationship to function? J Anat. 2009;214:258–66. https://doi.org/10.1111/j.1469-7580.2008.01020.x.
48. Fan F, Pabbidi MR, Ge Y, Li L, Wang S, Mims PN, Roman RJ. Knockdown of Add3 impairs the myogenic response of renal afferent arterioles and middle cerebral arteries. Am J Physiol Renal Physiol. 2017;312:F971–81. https://doi.org/10.1152/ajprenal.00529.2016.
49. Wang S, Jiao F, Border JJ, Fang X, Crumpler RF, Liu Y, Zhang H, Jefferson J, Guo Y, Elliott PS, et al. Luseogliflozin, a sodium-glucose cotransporter-2 inhibitor, reverses cerebrovascular dysfunction and cognitive impairments in 18-mo-old diabetic animals. Am J Physiol Heart Circ Physiol. 2022;322:H246–59. https://doi.org/10.1152/ajpheart.00438.2021.
50. Fan F, Sun CW, Maier KG, Williams JM, Pabbidi MR, Didion SP, Falck JR, Zhuo J, Roman RJ. 20-Hydroxyeicosatetraenoic acid contributes to the inhibition of K+ channel activity and vasoconstrictor response to angiotensin II in rat renal microvessels. PLoS One. 2013;8:e82482. https://doi.org/10.1371/journal.pone.0082482.
51. Pires PW, Jackson WF, Dorrance AM. Regulation of myogenic tone and structure of parenchymal arterioles by hypertension and the mineralocorticoid receptor. Am J Physiol Heart Circ Physiol. 2015;309:H127-136. https://doi.org/10.1152/ajpheart.00168.2015.
52. Lee RM. Morphology of cerebral arteries. Pharmacol Ther. 1995;66:149–73. https://doi.org/10.1016/0163-7258(94)00071-a.
53. Wang S, Tang C, Liu Y, Border JJ, Roman RJ, Fan F. Impact of impaired cerebral blood flow autoregulation on cognitive impairment. Front Aging. 2022;3:1077302. https://doi.org/10.3389/fragi.2022.1077302.
54 Fan F, Booz GW, Roman RJ. Aging diabetes, deconstructing the cerebrovascular wall. Aging (Albany NY). 2021;13:9158–9. https://doi.org/10.18632/aging.202963.
55. Marshall RS. Effects of altered cerebral hemodynamics on cognitive function. J Alzheimers Dis. 2012;32:633–42. https://doi.org/10.3233/jad-2012-120949.